THE ASTROPHYSICAL JOURNAL, 368:54–59, 1991 February 10

NEW VELOCITY DISPERSIONS AND PHOTOMETRY FOR E AND S0 GALAXIES IN THE GREAT ATTRACTOR

ALAN DRESSLER
The Observatories of The Carnegie Institution of Washington

S. M. FABER
University of California Observatories/Lick Observatory and Board of Studies in Astronomy and Astrophysics, University of California, Santa Cruz

AND

DAVID BURSTEIN
Department of Physics and Astronomy, Arizona State University, Tempe
Received 1990 January 25; accepted 1990 August 6

ABSTRACT

New spectroscopy and photometry have been obtained for 136 elliptical and S0 galaxies in the direction of the large-scale streaming flow attributed to the great attractor. Measurements of central velocity dispersion (σ), total B magnitudes (B_T), the photometric parameter D_n, and the absorption-line index Mg_2 are presented. Both internal and external comparisons indicate that measurements of log σ are accurate to 0.05 dex, B_T to 0.15 mag, D_n to 0.015 dex, and Mg_2 to 0.017 mag.

These data have been used in a previous paper by Dressler and Faber to estimate distances for these galaxies via the D_n-σ relation. It is shown in this paper that the D_n-Mg_2 relation also predicts the same trends of peculiar velocity with distance, but with less accuracy. The relative accuracy of other distance indicators for elliptical galaxies is also discussed.

Subject headings: galaxies: distances — galaxies: internal motions — galaxies: photometry

I. INTRODUCTION

Dressler and Faber (1990, hereafter DF) studied the field of peculiar velocities of elliptical and S0 galaxies in the direction of the great attractor (GA). Using techniques described in Dressler *et al.* (1987) and Lynden-Bell *et al.* (1988), distances to these galaxies were predicted using measured velocity dispersions and the photometric diameter D_n. DF confirmed earlier work showing a large-scale, large-amplitude flow in the direction $l = 307°$, $b = 9°$. In addition, support was provided for the great attractor model by showing that the peculiar velocities decline to zero at approximately the predicted distance of the center of the GA. Some evidence for infall to the backside was also found.

The principal purpose of this paper is to present the data on which the analysis of DF is based (§§ II and III) and to document the accuracy of these data (§ IV). A further examination of the use of the D_n-Mg_2 relation as a distance indicator, along with the efficacy of current distance indicators for ellipticals and S0's, is given in § V.

II. OBSERVATIONS

The Supergalactic Plane Redshift Survey (Dressler 1988, 1991) includes 1403 galaxies selected from the ESO catalog (Lauberts 1982) in the region $-30° < b < +45°$, $290° < l < 350°$ and larger than 1'.2 in diameter. The goal of DF was to obtain distances for E and S0 galaxies with observed velocities $V < 6500$ km s^{-1}. Using the ESO morphological classifications as a guide, DF inspected [on glass copies of the ESO (B) survey] approximately 200 galaxies and chose ~91 true ellipticals. Another ~48 galaxies were identified as E/S0 transition cases and large-bulge S0 galaxies. The extension of the D_n-σ relation to S0's and early-type spirals was proposed by Dressler (1987) and tested both by Lucey and Carter (1988) and with the present sample. Each of these studies has concluded that the D_n-σ relations for ellipticals and S0's have the same zero points and slopes within the errors of the samples. In order to mitigate the possibility of disk contamination, however, DF excluded edge-on and disk-dominated systems.

Spectra were taken of these 139 galaxies on 1988 March 11–16 and 1989 March 31–April 1, using the Modular Spectrograph built by Paul Schechter for the du Pont 2.5 m telescope at Las Campanas Observatory. A TI 800 × 800 × 15 μm CCD detector with a readout noise of $\sim 12e^-$ was used. An 85 mm camera produced a spatial resolution of 0.85 arcseconds per pixel; with a 1200 line mm^{-1} grating a wavelength coverage of 4850–6075 Å at 1.52 Å pixel^{-1} was achieved. Observations were made with a 2" slit, yielding a spectral resolution of ~3 Å FWHM, which provided a velocity resolution of $\sigma \sim 75$ km s^{-1}. Exposures of 200–2000 s resulted in typical signal-to-noise ratios S/N $\gtrsim$ 50 Å^{-1}. Template stars of type K0 III were observed in a similar manner except that the image was trailed and "wobbled" over the slit in order to illuminate the collimator in a manner similar to light from an extended source. The template observations were made to a S/N > 200 Å^{-1}.

Spectra were reduced from the two-dimensional frames using the software package Boroson's Astronomical Reduction Facility. Data reduction included the normal subtraction of bias levels and division by flat fields taken from exposures of the inside of the illuminated dome. After optical distortions were mapped and removed, sky subtraction was performed and spectra were extracted from a 5 pixel (~4") region centered on the nucleus of each galaxy. Wavelength calibration was done with hollow cathode/neon arcs taken after every group of about five galaxy spectra.

Velocity dispersions were measured in the Mg "b" band using a Fourier analysis program, described in Dressler (1984). One elliptical and two S0 galaxies were rejected because of strong emission in their spectra. Comparison of 105 repeat measurements of 39 program and five "standard" galaxies showed an internal error of 6% in the determination of the velocity dispersion, equivalent to the best data obtained by Davies *et al.* (1987). Aperture corrections referenced to the distance of the Coma Cluster were applied to the velocity dispersions, as described in Davies *et al.* These aperture corrections are small: for a typical galaxy at ~ 4000 km s^{-1}, the correction amounts to a decrease in the velocity dispersion by 0.012 in log σ, somewhat less than 3%.

Mg_2 values were measured from the spectra, following the definition given in Davies *et al.* A few galaxies per night, primarily intended as velocity dispersion standards, were also well-observed Mg_2 standards. Following the procedure outlined in Davies *et al.* and Faber *et al.* (1985), these were used to place the new data on the same photometric system. Night corrections, seven of which were <0.01 mag but one of which was 0.058 mag were made in order to place all the data on a common system.[1] Aperture corrections were applied to the Mg_2 values, as described in Davies *et al.* These aperture corrections are also small: for a typical galaxy at ~ 4000 km s^{-1}, the correction amounts to a decrease of Mg_2 of slightly more than 3%.

Photometric observations were made in Johnson B and I passbands with a TI 800 × 800 CCD at the Swope 1.0 m telescope on Las Campanas on seven nights: 1988 March 15–17, 1988 June 10, and 1989 March 31-April 2. The camera was operated in a 2 × 2 rebinning mode, which produced a field size of ~ 6 arcmin^2 at 0$''$87 pixel^{-1}. Most B exposures were 200 s; for some of the brighter galaxies, the integration time was cut to 120 s to avoid saturation of the nucleus. Flat-field exposures were taken of the twilight sky; medians of these frames were made in order to remove star images. These flat-field exposures contained $\sim 10^4$ counts per pixel, well above the average exposure level of 10^3 counts per pixel for the galaxy (typically spread over ~ 1000 pixels) and ~ 250 counts for the sky value. The resulting frames are usually flat to ± 1%, although scattered light from bright stars sometimes results in irregularities which lead to greater uncertainty, but never more than ± 3%. These numbers suggest that uncertainties in the magnitudes from counting statistics and these sources of systematic error are $\lesssim 0.01$ mag.

External comparisons with B_T and D_n values, discussed below, confirm that the effect of errors in flat fielding and sky subtraction on the derivation of the photometric parameters is small. In a separate paper, we will employ a new luminosity profile-fitting program developed by E. Bertschinger to study the form of the brightness profile of elliptical galaxies, which can be used to explicitly estimate these errors if the galaxy truly follows an $r^{1/4}$ law luminosity distribution.

Several fields, each containing a sequence of stars with measured fluxes (Graham 1982), were observed many times during the night. These verified the photometric quality of each night and provided extinction coefficients over a range of air masses bracketing the galaxy observations. Five cloudless nights were confirmed to be photometric. Of particular concern, however, were the nights of 1988 March 15 and March 16, during which an unusually thick haze covered Las Campanas. Our reductions of 12 standard fields on May 15 and seven fields on May 16 confirmed that the B extinctions were much higher than average by 0.2 and 0.4 mag, respectively. However, the scatter in zero point was no greater than for observations during the other five nights; hence, we concluded that these nights could be treated as photometric. Analysis of the zero-point stability through each of the seven nights indicated slow drifts of $\lesssim 0.1$ mag. When larger than 0.05 mag, these were removed by fitting the time variation with a second-order polynomial. (Such temporal variations in nightly extinction are not limited to Las Campanas, but have been seen at Kitt Peak National Observatory as well [D. B., unpublished data]). Typical rms errors of the standard stars were 0.02 mag. Color corrections of $\lesssim 0.01$ mag were implied by the photometric transformations, but these have not been applied because at this level they were poorly defined and were, in any case, comparable to other sources of systematic and random error.

After standard reduction of these CCD frames using the Boroson programs, the B galaxy frames were converted to a form acceptable by the Cassandra data reduction program, written by Don Schneider and Peter Young. (The I frames were processed, but no data have been extracted from them, as of this writing.) With Cassandra, sky levels were measured and contaminating stars removed. The integral and differential luminosity profiles for each galaxy were obtained by summing counts within circular apertures centered on the galaxy out to typical radii of 1′–2′, at which point the observed surface brightness was a few percent of sky. The magnitude within the 23rd mag arcsec^{-1} isophote was extracted and converted into a total B magnitudes using $B_T = B_{\mu<23} - 0.57$, a statistical correction based on the standard growth curve (see Burstein *et al.* 1987). Although our error analysis indicates that the rms errors in B_{23} should be $\lesssim 0.03$ mag, larger errors may be found in comparison of our B_T values to those of other sources, as discussed below. As is typical for galaxy photometry, such discrepancies are as likely due to differences in the method of extrapolation to a total magnitude as much as (or more than) differences in the measurements themselves.

III. THE CATALOG

Table 1 presents the cataloged data. Column (1) is the number in the SPS survey (Dressler 1990). Column (2) gives the NGC or IC number if the galaxy is so cataloged; otherwise, the ESO catalog number is given. Column (3) is the type, E or S0, as determined by us from inspection of glass copies of the ESO (B) survey. The group number assigned by Burstein, Faber, and Dressler (1990), if any, is given in column (4); the corresponding heliocentric group velocity is given in column (6). Column (5) lists the heliocentric velocity as determined in this study. Column (7) gives the B-band Galactic extinction, A_B, taken from Burstein and Heiles (1984) as modified by Burstein, Faber, and Dressler. The total blue magnitude, B_T, is given in column (8). Column (9) gives log D_n, in units of 0$'$1. Column (10) gives log σ in km s^{-1}, and column (11) lists values of Mg_2. The D_n values here have been corrected for K-dimming and Galactic extinction as in Faber *et al.* (1989). However, the B_T values are raw and require these two corrections before comparison can be made to the photometric catalogs of Burstein *et al.* (1987) and Faber *et al.*

[1] The one large correction, for 1989 April 1, was due to the loss of flat-field exposures due to a taping error. Use of flat fields from the previous night resulted in an improper continuum shape that introduced the large zero-point correction. After application of the large zero-point correction, the accuracy of these measurements was found to be as high as the other nights. For example, there were 25 galaxies observed on this night which had also been observed in 1988 March. Comparison of these Mg_2 values showed a rms dispersion in the differences of only 0.012 mag.

TABLE 1

DATA

SPS #	Name	Type	Gr. #	V	V_g	A_B	B_T	log D_n	log σ	Mg_2
8	E005-G007	E	22	5384	5260	0.57	14.79	0.45	2.120	0.222
9	E005-G010	E	22	5132	5260	0.51	13.59	0.66	2.452	0.322
60	IC 2977	E		2906		0.37	13.20	0.66	2.304	0.252
77	E267-G011	E		4545		0.50	13.94	0.52	2.245	0.290
80	E171-G008	E		4441		0.50	13.85	0.57	2.426	0.313
85	NGC 4087	E		3296		0.48	13.09	0.73	2.362	0.295
92	NGC 4105	E	49	1864	2020	0.24	11.57	0.98	2.418	0.308
93	NGC 4106	E	49	2163	2020	0.24	12.10	0.89	2.246	0.275
100	IC 3010	S0	49	2000	2020	0.21	13.23	0.56	1.965	0.238
137	IC 3152	E		3274		0.43	13.06	0.75	2.211	0.246
143	E218-G002	S0		4287		0.39	13.83	0.56	2.366	0.312
161	NGC 4373	E	35	3367	3320	0.37	11.81	0.97	2.359	0.286
162	E268-G004	E		5234		0.40	13.42	0.63	2.451	0.330
170	IC 3370	E	35	2969	3320	0.33	12.07	0.89	2.263	0.267
203	E322-G038	S0	58	3134	3041	0.51	13.69	0.64	2.301	0.313
219	E322-G051	S0	58	3216	3041	0.51	13.69	0.61	2.234	0.315
230	E322-G059	S0		3295		0.30	13.44	0.49	2.353	0.309
231	NGC 4645B	S0	58	2641	3041	0.50	13.11	0.75	2.203	0.312
233	NGC 4645	E	58	2574	3041	0.50	12.71	0.83	2.279	0.294
248	E322-G075	S0	59	4520	4570	0.49	13.76	0.61	2.160	0.264
254	NGC 4696B	E	58	3058	3041	0.47	13.48	0.68	2.398	0.282
263	NGC 4696D	S0	58	2606	3041	0.47	13.58	0.65	2.198	0.277
268	NGC 4696	E	58	3010	3041	0.46	11.60	0.92	2.438	0.287
271	NGC 4706	S0	58	3807	3041	0.46	13.65	0.63	2.367	0.316
273	NGC 4709	E	59	4654	4570	0.47	12.62	0.81	2.419	0.337
285	E507-G025	E		3157		0.29	12.35	0.84	2.376	0.296
290	E323-G015	S0	58	3103	3041	0.33	14.16	0.46	2.149	0.245
291	NGC 4729	E	58	3285	3041	0.42	13.45	0.66	2.197	0.289
295	E323-G019	S0	58	3859	3041	0.46	14.01	0.58	2.088	0.252
298	NGC 4743	S0	58	2959	3041	0.46	13.73	0.59	2.074	0.262
299	E575-G013	E		6893		0.16	14.12	0.47	2.448	0.313
302	E323-G023	S0	59	4416	4570	0.42	14.14	0.50	2.163	0.294
311	E323-G024	E	59	4277	4570	0.41	12.86	0.81	2.376	0.298
316	NGC 4767	E	58	2934	3041	0.41	12.53	0.85	2.324	0.296
327	E507-G045	E	28	4826	4701	0.33	12.97	0.73	2.500	0.308
328	E507-G046	E	28	4574	4701	0.35	14.03	0.50	2.245	0.283
332	IC 3896	E		2022		0.50	12.24	0.84	2.364	0.320
341	NGC 4830	E		3290		0.17	12.88	0.69	2.231	0.262
342	NGC 4831	E		3139		0.36	13.49	0.61	2.178	0.284
359	E575-G043	E		6877		0.28	13.86	0.52	2.372	0.270
367	E443-G024	E	275	5107	4868	0.30	12.82	0.74	2.447	0.291
368	E381-G047	E		4796		0.13	14.47	0.35	2.227	0.298
374	E443-G032	E	275	4575	4868	0.35	13.10	0.73	2.473	0.297
390	IC 844	S0	37	2852	3269	0.34	13.34	0.69	2.101	0.214
395	E443-G043	E	37	3558	3269	0.34	13.95	0.55	2.047	0.235
396	NGC 4936	E	37	3222	3269	0.34	11.99	0.93	2.447	0.296
402	NGC 4946	E	62	3033	3251	0.41	13.29	0.70	2.300	0.298
404	NGC 4955	E	37	3449	3269	0.35	13.06	0.65	2.318	0.332
412	IC 4180	S0	38	2865	3009	0.29	13.68	0.56	1.823	0.190
421	NGC 4970	E	38	3176	3009	0.29	13.16	0.67	2.292	0.270
424	IC 4197	E	38	2979	3009	0.29	13.53	0.59	2.274	0.286
427	NGC 4976	E		1415		0.35	10.85	1.23	2.145	0.233
434	E040-G002	E		2896		0.35	13.87	0.48	2.241	0.310
444	E323-G089	S0		2866		0.34	13.22	0.65	2.351	0.327
453	NGC 5011	E	62	3096	3251	0.40	12.30	0.89	2.425	0.288
457	NGC 5018	E	63	2716	2733	0.22	11.61	1.02	2.281	0.191
462	E269-G072	E	62	2950	3251	0.46	14.01	0.56	2.318	0.266
479	NGC 5048	E	37	4322	3269	0.25	13.65	0.59	2.266	0.238
492	E382-G034	S0		3407		0.18	13.55	0.58	1.940	0.239
495	NGC 5061	E	274	2015	2034	0.25	11.13	1.10	2.311	0.257
502	E269-G080	E		3059		0.35	13.45	0.58	2.237	0.304
506	IC 874	S0	274	2262	2034	0.21	13.42	0.61	2.085	0.222
508	NGC 5090A	E	65	3431	3828	0.48	13.79	0.58	2.253	0.272
525	NGC 5087	E	274	1821	2034	0.29	11.78	0.95	2.458	0.328
526	NGC 5082	S0	65	3910	3828	0.48	13.86	0.55	2.287	0.330
532	NGC 5090	E	65	3406	3828	0.48	12.10	0.83	2.417	0.324
545	NGC 5114	E	64	3583	3713	0.18	13.34	0.64	2.272	0.267
551	NGC 5124	S0	88	4085	4148	0.20	12.99	0.70	2.388	0.314
563	NGC 5140	E	64	3847	3713	0.17	12.74	0.69	2.290	0.258
580	NGC 5153	E	88	4203	4148	0.21	13.19	0.65	2.251	0.296
598	E576-G067	S0		5590		0.21	14.06	0.47	2.252	0.249
612	NGC 5193	E	64	3651	3713	0.15	12.82	0.72	2.361	0.297
641	IC 4293	E		4569		0.26	13.70	0.56	2.385	0.312
644	IC 4296	E	64	3690	3713	0.12	11.73	0.92	2.524	0.317
692	E509-G008	S0		5863		0.25	14.08	0.51	2.420	0.299
701	IC 4329	E	66	4515	4508	0.14	12.49	0.68	2.452	0.325
708	NGC 5304	E	66	3671	4508	0.15	13.69	0.53	2.311	0.280
728	NGC 5328	E	66	4684	4508	0.16	12.40	0.79	2.517	0.302
735	NGC 5333	S0		2789		0.50	12.01	0.86	2.251	0.286
744	E384-G013	E	76	3708	4030	0.21	13.99	0.45	1.916	0.195
745	NGC 5357	E	66	4822	4508	0.18	13.04	0.70	2.349	0.253
754	E384-G019	S0	76	4188	4030	0.21	13.57	0.57	2.162	0.275
755	NGC 5365	S0		2403		0.33	12.28	0.90	2.355	0.316
768	NGC 5397	S0	76	4061	4030	0.22	13.73	0.55	2.383	0.294
785	NGC 5419	E	76	4107	4030	0.23	12.01	0.88	2.502	0.337
813	E221-G026	E		1353		0.40	11.94	0.96	2.107	0.251
839	NGC 5516	E		4365		0.50	13.08	0.70	2.513	0.327
854	E511-G023	E	276	6656	7180	0.27	13.87	0.53	2.429	0.287
861	E446-G049	E		3784		0.40	13.91	0.51	2.130	0.256
873	E385-G017	E		3947		0.29	14.02	0.51	2.167	0.273
887	IC 4421	E		3602		0.33	13.31	0.67	2.274	0.270
908	IC 4451	E	40	4170	4259	0.23	13.23	0.64	2.363	0.316
909	IC 4453	S0		3547		0.43	12.74	0.80	2.201	0.227
912	NGC 5670	S0		2883		0.35	12.74	0.77	2.205	0.200
916	IC 4464	S0	40	4346	4259	0.29	13.18	0.66	2.227	0.292
938	E512-G018	S0	69	3484	3447	0.39	12.97	0.65	2.283	0.286
954	E580-G026	S0	69	3314	3447	0.35	14.75	0.32	1.959	0.135
962	NGC 5761	S0	69	4074	3447	0.37	13.57	0.61	2.269	0.291
963	E580-G040	E	69	4116	3447	0.38	14.34	0.48	2.239	0.277
972	E386-G031	S0		6230		0.26	14.66	0.40	2.429	0.304
982	E386-G041	E		4083		0.26	13.45	0.64	2.278	0.268
992	NGC 5791	E	69	3277	3447	0.35	12.57	0.81	2.385	0.311
1002	E581-G016	S0	69	4090	3447	0.34	13.37	0.68	2.226	0.245
1005	NGC 5799	S0		3053		0.35	13.32	0.59	2.118	0.239
1041	NGC 5898	E	71	2076	2321	0.48	12.25	0.91	2.325	0.287
1043	NGC 5903	E	71	2516	2321	0.45	12.37	0.84	2.299	0.300
1120	E137-G006	E	42	5421	4200	0.95	12.68	0.84	2.582	0.307
1121	E137-G008	E	42	3791	4200	0.95	12.23	0.90	2.417	0.305
1122	E137-G010	E	42	3380	4200	0.95	12.42	0.69	2.311	0.292
1146	E069-G014	E		4743		0.45	12.67	0.83	2.362	0.257
1168	NGC 6305	S0		2675		0.50	12.99	0.78	2.233	0.251
1196	NGC 6407	E	81	4578	4423	0.35	13.40	0.66	2.445	0.317
1206	E139-G045	E	81	4292	4423	0.40	13.66	0.62	2.369	0.297
1228	NGC 6557	S0		5558		0.72	13.76	0.63	2.352	0.272
1240	IC 4704	E	79	3552	3401	0.09	12.80	0.71	2.405	0.301
1242	E071-G013	S0	79	3238	3401	0.30	13.61	0.54	2.119	0.240
1248	IC 4718	S0	67	3806	4200	0.30	13.57	0.59	2.079	0.240
1262	IC 4742	E	67	4391	4200	0.32	12.95	0.60	2.320	0.301
1265	NGC 6653	E		5185		0.28	13.28	0.64	2.328	0.271
1269	NGC 6673	S0	78	1152	1009	0.31	12.22	0.88	2.153	0.257
1270	IC 4765	E	67	4467	4200	0.29	13.37	0.65	2.463	0.332
1271	IC 4767	S0	67	3519	4200	0.29	14.59	0.32	2.099	0.247
1274	NGC 6684	S0	78	866	1009	0.23	11.89	0.83	2.033	0.231
1282	E104-G020	S0	67	4863	4200	0.22	13.58	0.55	2.406	0.309
1291	IC 4797	E	279	2611	2651	0.29	12.09	0.93	2.357	0.302
1302	NGC 6721	E	67	4355	4200	0.26	13.03	0.70	2.455	0.321
1313	NGC 6733	E	67	4884	4200	0.22	13.38	0.59	2.376	0.310
1325	NGC 6746	E	67	4189	4200	0.16	13.71	0.49	2.400	0.273
1339	NGC 6758	E	74	3445	3416	0.19	12.51	0.80	2.419	0.317
1354	IC 4842	S0	67	4183	4200	0.17	13.46	0.54	2.281	0.282
1365	NGC 6776	E		5428		0.19	12.94	0.72	2.306	0.245
1377	E105-G004	E	67	4035	4200	0.25	13.79	0.55	2.356	0.317
1379	E184-G078	E	74	3359	3416	0.14	13.45	0.56	2.192	0.243
1382	E105-G007	S0	67	4340	4200	0.30	14.49	0.41	2.335	0.288
1386	IC 4864	S0		5851		0.42	15.13	0.20	2.290	0.261
1398	IC 4889	E	77	2480	2325	0.18	11.98	0.89	2.194	0.259

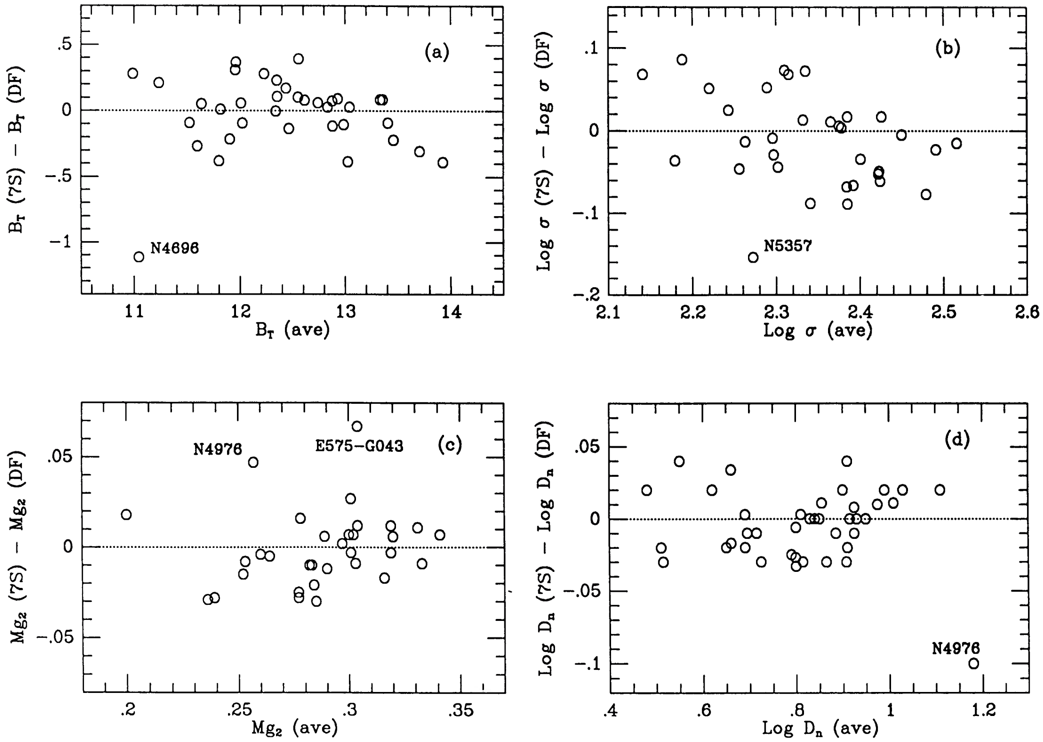

FIG. 1.—Comparison of data common to DF and 7S studies for B_T (Fig. 1*a*), log σ (Fig. 1*b*), Mg_2 (Fig. 1*c*), and log D_n. In each case the difference is plotted vs. the average of the two studies. Zero-points and scatter are given in the text.

Table 1 is available in machine readable form from D. B. at e-mail address burstein@asucps.bitnet.

IV. DATA COMPARISONS

Many of the galaxies in the present survey were also observed in the seven Samurai (7S) survey (Davies *et al.* 1987; Burstein *et al.* 1987; Faber *et al.* 1989). Figures 1*a*–1*d* show the comparisons between the present data and those of the 7S survey for B_T, log σ, Mg_2, and D_n. In each case, the difference (7S − DF) is plotted versus the average value (7S + DF)/2.

The comparison of B_T values shows a scatter of 0.21 mag and a negligible zero-point offset of 0.009 ± 0.035 mag for 35 of the 36 galaxies in common (restricting the 7S sample to data of quality "2" or better). This is compatible with the estimated error of 0.15 mag in the Burstein *et al.* magnitudes alone. For one galaxy, NGC 4696, the DF measurement of 11.60 is 1.1 mag fainter than the 7S value but is consistent with the value of 11.75 listed in the Second Reference Catalog (de Vaucouleurs, de Vaucouleurs, and Corwin 1976). Upon examination of the luminosity profile given for this galaxy in Figure 3 of Burstein *et al.*, it appears likely that the B_T value given there is in error, probably the result of a large extrapolation of photoelectric photometry through small apertures. The galaxy is the cD in the cluster Cen 30 and has a very extended, diffuse profile.

An additional comparison can be made with the B_T values of Lauberts and Valentijn (1989), who determined magnitudes and diameters for most of the ESO galaxies from scans of photographic plates. As shown in Figure 2, the zero-point difference between ESO and DF is only 0.06 ± 0.02 mag, in the sense that the DF values are brighter. The scatter of 0.18 mag in Figure 2 implies a 0.13 mag rms error for each data set if the errors are equally shared.

The comparison of log σ between 7S and the present data (Fig. 1*b*) shows a scatter of less than 0.05 dex for 32 of 33 galaxies, with a zero-point shift of only 0.008 dex (1.86%) ± 0.009 dex, in the sense that the 7S velocity dispersions are marginally smaller. Adopting the accuracy of 0.04 dex quoted for the 7S data which were multiply observed, the comparison implies an accuracy of 0.03 dex for the present determinations of log σ, comparable to the accuracy of 0.025 dex for these data, as estimated from internal comparisons (see § II). The zero-point shift corresponds to distance error of only 2.2% using the D_n-σ relation, or 134 km s^{-1} at 6000 km s^{-1}, the limit of the DF sample. A zero-point difference of similar size and of

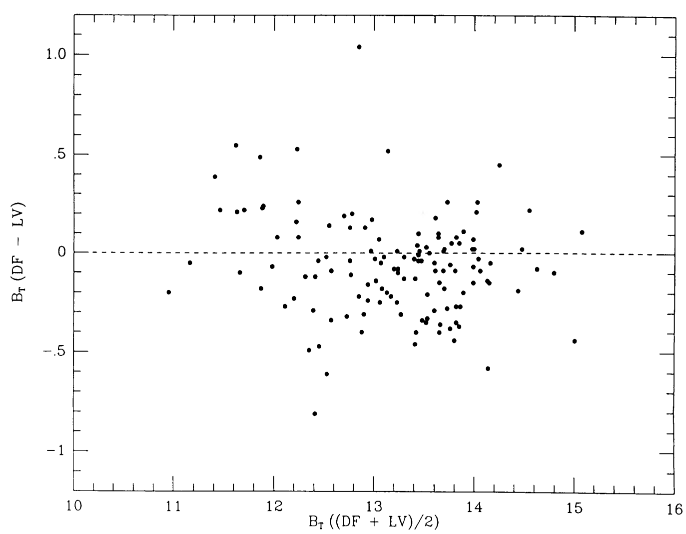

FIG. 2.—Comparison of the B_T magnitudes in this study with photographically determined values from Lauberts and Valentijn (1989).

the same sense was also found by Lucey and Carter (1988). There is also a suggestion that this systematic difference is a function of velocity dispersion, although the effect is marginal. The consequences of this trend, if real, on the measurement of peculiar velocities should be below the 100 km s^{-1} level over the region of interest, since the full range of the effect is washed out by the spread in velocity dispersions at any given distance.

The one galaxy for which the value of log σ is highly discrepant, NGC 5357, was observed only once in the 7S survey, and the 0.15 dex difference between 7S and DF is only a 2 σ variation in this particular case (combined error of 0.07 dex). As both the zero-point difference and possible systematic trend are small compared to the observed scatter, no correction has been made for the data presented here or used in DF.

Mg_2 measurements are compared for 32 galaxies in common between 7S and DF in Figure 1*c*. For 30 of the galaxies, the rms dispersion in the differences is 0.015 mag, with a negligible zero-point shift of 0.005 ± 0.003 mag. The two most discrepant galaxies are NGC 4975 and ESO 0575–G043 with residuals of 0.05–0.06 mag. A small systematic trend may be present, in the sense that 7S Mg_2 values are $\sim$0.015 mag smaller than DF values for relatively weak-lined galaxies.

Finally, D_n values are compared in Figure 1*d*. It is satisfying to note that, as D_n was designed to be a photometric parameter for which reliable measurement is relatively easy, there are no systematic trends in the comparison, a negligible zero-point shift (-0.003 ± 0.003 dex), and a combined scatter of 0.020 dex for 40 of 41 galaxies in common. (No obvious reason could be found for the anomalous discrepancy for NGC 4976.) The error in measuring distances implied by this zero-point shift is only 42 km s^{-1} at 6000 km s^{-1}. Assuming equal errors for both 7S and DF, this comparison implies an error of 0.014 dex per source. This random error would limit the measurement of distance to an accuracy of 3.3%, but in fact the intrinsic scatter of the D_n-σ relation is roughly 6 times as large.

In summary, we conclude that the photometric parameters B_T and D_n are equivalent to the quality " 1 " data of 7S and on the same photometric system. Mg_2 and log σ measurements are also on the system of 7S to a level of <2% and <1% respectively, with scatter equivalent to the best data obtained by 7S. The offsets and trends found in comparing the data sets imply small systematic distance errors of $\lesssim 100$ km s^{-1}.

V. THE ACCURACY OF D_n-Mg_2 AND OTHER DISTANCE INDICATORS

It is of interest to investigate whether any of the other intrinsic properties of ellipticals can be used as distance indicators of accuracy comparable to the D_n-σ relation. The word "comparable" is key here, because the dominant systematic errors in distance determinations, the Malmquist-like bias, increases as the square of the random error for a uniformly distributed sample.

Terlevich *et al.* (1981) showed that Mg_2 and log σ are strongly correlated for elliptical galaxies of similar luminosity. Thus, Dressler (1984) and Dressler *et al.* (1987) investigated the use of Mg_2 in place of log σ in distance-dependent relations. In view of the current discussion of the use of distance indicators for ellipticals (de Carvalho and Djorgovski 1989; Lynden-Bell *et al.* 1989), we feel it is worthwhile to address this issue once more, using the present data. In addition, as the errors in the D_n-Mg_2 relation are partly independent of those in the D_n-σ relation, such an investigation provides another view of the large-scale motions in the direction of the great attractor.

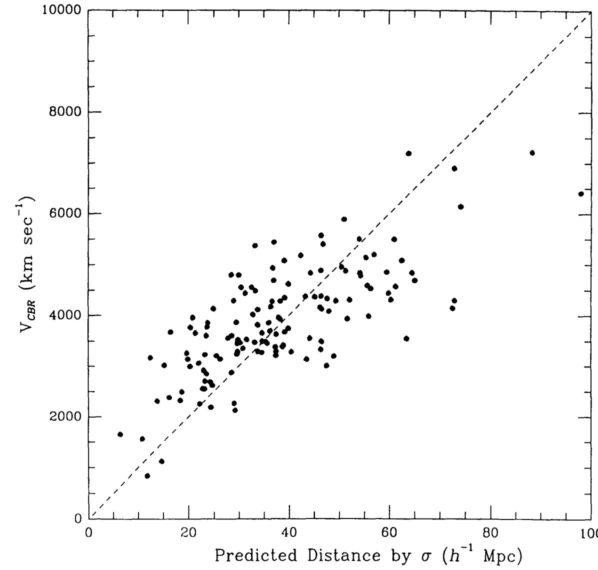

FIG. 3.—Hubble diagram toward the great attractor for galaxies in DF, based on the D_n-σ relation. The data include a correction for a Malmquist-like bias in the case of uniform density, adopting an rms error of 21% in distance for each galaxy.

Figures 3 and 4 compare the Hubble diagrams made with the D_n-σ and D_n-Mg_2 relations, respectively. The D_n-σ relation is of the form log $D_n \sim 1.2$ log σ (DF), while the D_n-Mg_2 relation is of the form log $D_n \sim 6.33$ log Mg_2 (Dressler *et al.* 1987). Zero-points for both relations are given by the respective relations observed for galaxies in the Coma cluster, in keeping with the methodology used in DF and 7S. Corrections for Malmquist-like bias are applied to these data, following Lynden-Bell *et al.* (1988), with rms distance errors of 21% and 30% used for D_n-σ and D_n-Mg_2, respectively. The estimate of

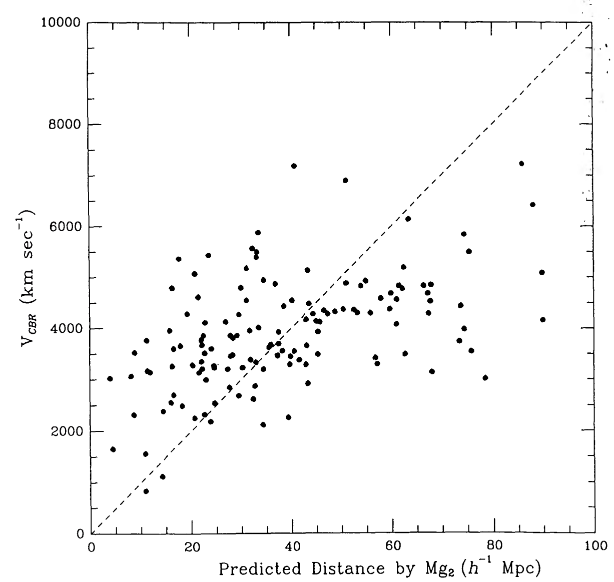

FIG. 4.—Same as Fig. 3, except that distances have been predicted using the D_n-Mg_2 relation. The data again include a correction for a Malmquist-like bias for which an rms error of 30% has been adopted. The resemblance of Fig. 4 to Fig. 3 supports the interpretation that distances can be predicted with the D_n-Mg_2 relation but with typical errors $\sim$50% larger than those determined with the D_n-σ relation.

30% for the scatter in D_n-Mg_2 is less than the 38% found by Dressler *et al.* (1987) for galaxies in four clusters.

That Figures 3 and 4 show the same trend—the large outflow for $D < 35h^{-1}$ Mpc and the crossing of the line corresponding to an unperturbed Hubble flow at $D \sim 45h^{-1}$ Mpc—is encouraging, confirming previous analyses that showed the D_n-Mg_2 relation yields distances consistent with the D_n-σ relation. Furthermore, the resemblance of Figures 3 and 4 confirms with a different method the conclusions of DF concerning deviations from a uniform Hubble flow. Unfortunately, the larger scatter in the D_n-Mg_2 relation means that it can only be used to provide a consistency check of the large-scale velocity field as obtained from the more accurate D_n-σ relation.

Lynden-Bell *et al.* (1989) sought the "best" distance indicator by combining in various combinations seven parameters observed by 7S for ellipticals in the Coma and Virgo Clusters. These parameters were log σ, effective surface brightness μ_e, ratio of D_n to isophotal diameter, Mg_2, $B-V$, surface brightness at D_n, and axial ratio. No combination of these parameters gave significantly better distances than the use of the D_n-σ relation alone. For 50 galaxies in these two clusters, Lynden-Bell *et al.* find a distance error of only 17%, about 25% smaller than the average of 21% for the 7S data set as a whole.

De Carvalho and Djorgovski (1989, hereafter DD) have also examined the accuracy of several parameters of ellipticals as distance indicators. Their analysis differs from that of Lynden-Bell *et al.* in regard to choice of parameters and in the fact that DD examined only three-parameter relations. The parameters used included effective radius r_e, absolute magnitude, μ_e, $B-V$, $U-R$, $V-K$, and Mg_2. The galaxies used by DD come primarily from the Virgo and Coma Clusters and, as such, should be directly comparable to those of Lynden-Bell *et al.*

It is also worth noting that Burstein *et al.* (1989) show that $B-V$ color and Mg_2 are related on a one-to-one basis for ellipticals, and that previous investigators have shown that all optical and IR colors are strongly correlated (e.g., Aaronson 1977).

Of the 15 different combinations of parameters investigated by DD, only one set (Mg_2, μ_e) has a distance error (15%) comparable to the D_n-σ relation. Their relation yields a distance error of 15% for 16 Virgo galaxies and 20% for 22 Coma galaxies. This should be compared to the 17% that Lynden-Bell *et al.* find for these clusters from the D_n-σ relation. All of the other relations investigated by DD have errors ranging from 21% to 38%. The D_n-Mg_2 relation used here to derive the distances in Figure 4 is a typical representative of this family. Thus, none of the relations proposed for elliptical galaxies predict distances significantly better than that of the D_n-σ relation, and most of them are considerably worse.

We conclude that, in the context of these parameters, the D_n-σ relation is still the relationship of choice for determining distance to elliptical galaxies, given both the accuracy to which the D_n parameter can be easily measured and the fact that the systematic errors introduced by Malmquist-like bias increase as the square of the random error.

The authors thank Paul Schechter and Ian Thompson for building the spectrograph and detector used in this study, and the staff of Las Campanas Observatory, particularly Oscar Duhalde, for helping with the observations. The authors acknowledge the National Science Foundation for support through grants AST-8715260 (AD) and AST-8702894 (SMF).

REFERENCES

Aaronson, M. 1977, Ph.D. thesis, Harvard University.
Burstein, D., Davies, R. L., Dressler, A., Faber, S. M., Lynden-Bell, D., Terlevich, R. J., and Wegner, G. 1989, in *Large Scale Structure and Motions in the Universe*, ed. M. Messetti *et al.* (Dordrecht: Kluwer), p. 179.
Burstein, D., Davies, R. L., Dressler, A., Faber, S. M., Stone, R. P. S., Lynden-Bell, D., Terlevich, R. J., and Wegner, G. 1987, *Ap. J. Suppl.*, **64**, 601.
Burstein, D., Faber, S. M., and Dressler, A. 1990, *Ap. J.*, **354**, 18.
Burstein, D., and Heiles, C. 1984, *Ap. J. Suppl.*, **54**, 33.
Davies, R. L., Burstein, D., Dressler, A., Faber, S. M., Lynden-Bell, D., Terlevich, R. J., and Wegner, G. A. 1987, *Ap. J. Suppl.*, **64**, 581.
de Carvalho, R. R., and Djorgovski, S. 1989, *Ap. J.* (*Letters*), **341**, L37 (DD).
de Vaucouleurs, G., de Vaucouleurs, A., and Corwin, H. G. 1976, *The Second Reference Catalog of Bright Galaxies* (Austin: University of Texas).
Dressler, A. 1984, *Ap. J.*, **281**, 512.
———. 1987, *Ap. J.*, **317**, 1.
———. 1988, *Ap. J.*, **329**, 519.
———. 1991, *Ap. J. Suppl.*, in press.
Dressler, A., and Faber, S. M. 1990, *Ap. J.*, **354**, 13 (DF).
Dressler, A., Lynden-Bell, D., Burstein, D., Davies, R. L., Faber, S. M., Terlevich, R. J., and Wegner, G. 1987, *Ap. J.*, **313**, 42.
Faber, S. M., Friel, E. D., Burstein, D., and Gaskell, C. N. 1985, *Ap. J. Suppl.*, **57**, 711.
Faber, S. M., Wegner, G., Burstein, D., Davies, R. L., Dressler, A., Lynden-Bell, D., and Terlevich, R. J. 1989, *Ap. J. Suppl.*, **69**, 763.
Graham, J. A. 1982, *Pub A.S.P.*, **94**, 244.
Lauberts, A. 1982, *The ESO/Uppsala Survey of the ESO* (*B*) *Atlas* (ESO: Garching bei München).
Lauberts, A., and Valentijn, E. A. 1989, *Surface Photometry of the ESO-Uppsala Galaxies* (ESO: Garching bei München).
Lucey, J. R., and Carter, D. 1988, *M.N.R.A.S.*, **235**, 1177.
Lynden-Bell, D., Faber, S. M., Burstein, D., Davies, R. L., Dressler, A., Terlevich, R. J., and Wegner, G. 1988, *Ap. J.*, **326**, 19.
Lynden-Bell, D., Burstein, D., Davies, R. L., Dressler, A., Faber, S. M., Terlevich, R. J., and Wegner, G. 1989, in *The Extragalactic Distance Scale*, ed. S. van den Bergh and C. Pritchet (Provo: Astronomical Society of the Pacific), p. 307.
Terlevich, R., Davies, R. L., Faber, S. M., and Burstein, D. 1981, *M.N.R.A.S.*, **196**, 381.

DAVID BURSTEIN: Department of Physics and Astronomy, Arizona State University, Tempe, AZ 85287-1504

ALAN DRESSLER: The Observatories of the Carnegie Institution of Washington, 813 Santa Barbara Street, Pasadena, CA 91101-1292

S. M. FABER: University of California Observatories/Lick Observatory and Board of Studies in Astronomy and Astrophysics, University of California, Santa Cruz, CA 95064